

Collimator Simulation for the TRIUMF KAON Factory using DIMAD

U. Wienands, C.P. Parfitt*, and F.W. Jones

TRIUMF, 4004 Wesbrook Mall, Vancouver, B.C., Canada V6T 2A3

Abstract

A collimator-element routine has been developed for the lattice and tracking code DIMAD, to facilitate simulation of the beam collimation system for the TRIUMF KAON Factory accelerators. Multiple Coulomb scattering, energy loss, and elastic nuclear scattering are simulated, and the fraction of particles undergoing inelastic nuclear events is estimated. The routines are accurate over a large energy range, up to about 1 TeV. Results for the beam collimation system of the KAON Factory Booster synchrotron are presented.

I. INTRODUCTION

Collimators and scrapers are used in synchrotrons and storage rings to shape the beam as well as localize the losses inevitably occurring during routine operation. For the KAON Factory accelerators the localization of losses is mandatory, due to the high average beam currents involved, if hands-on maintenance is to be feasible even after years of operation.

The primary figure of merit for a beam collimation system is its collection efficiency, *i.e.* the ratio of the number of particles captured in the actual absorbers to the total number of particles intercepted by them, the remainder being lost in a more or less distributed fashion around the ring. To get a realistic estimate of this number the scattering processes of particles traversing a block of material have to be simulated. We have developed a set of routines for this purpose, to be included as a special collimator element in the lattice and tracking code DIMAD. [1] These routines model multiple scattering, energy loss, and elastic nuclear events. The cross section for inelastic nuclear events is also estimated, but particles undergoing inelastic nuclear events are considered lost at that point. By incorporating the collimators in DIMAD simulations can easily be carried out for realistic scenarios, *i.e.* tracking in three dimensions, with rf, etc. Another potential use of the routines is the simulation of gas targets in storage rings in order to determine the beam life time and the background generated by scattering in the target. Beam particles are presently limited to protons.

As the outscattering from the absorbers back into the aperture of the ring can be considerable, beam collimation is done in at least two stages. A primary collimator defines the acceptance and a secondary collimator catches the particles scattered off the first collimator. The outscattering rate depends strongly on the distance from the face at which particles hit the absorber and on the angle of the incident particles, both of which will be large for particles

scattered off the first collimator and hitting the second one; therefore the secondary collimator will have a small outscattering rate. If the collimators are effective in one plane only, two secondary collimators may be necessary, one for each plane, since the outscattering from the primary collimator is not limited to one plane. Preferably the secondary collimator(s) will be 90° in phase away from the primary collimator to maximize the efficiency.

In this paper the issue of shielding around the collimator location is not addressed. However, in addition to the overall collimation efficiency we can determine which elements in the ring get irradiated as a result of the residual distributed losses. The routines discussed here are in part modifications of routines used in a code simulating H⁻ injection and storage of protons in the KAON Factory Accumulator ring [2].

II. THE COLLIMATOR ELEMENT

The collimator is implemented as an *arbitrary element* in DIMAD. As long as particles do not hit the absorbers they are transported as in a drift region. When a particle hits the absorber either grazing the face or head-on onto the leading edge the part of the absorber still in front of the particle is subdivided into slices and the particle is transported from slice to slice. At the centre of each slice the particle's coordinates x' , y' and dp are updated to reflect the effects of multiple scattering, energy loss, and elastic nuclear scattering.

A. Multiple scattering

Multiple scattering is simulated using a modified version of the CERN library routine MLR, implementing Molière's theory [3]. The scattering angle generated is projected onto the x' , y' plane and added to the respective particle's coordinates. This small-angle approximation is justified as the scattering angles are typically less than 10 mr per slice.

B. Energy loss

The mean energy loss per slice is calculated using the well known Bethe-Bloch formula. Individual values for δE are then picked from either a Landau or a Gaussian distribution, depending on the thickness of the slice. A Vavilov distribution is also implemented using the CERN routine DINVAV [4]; however, computing time for the Vavilov routine proved to be prohibitive for multi tracking because the routine has to be initialized for each energy, *i.e.* each slice. The distribution used can be controlled by a parameter in the element definition.

*Simon Fraser University, Burnaby, B.C.

C. Nuclear scattering

For nuclear events a total cross section dependent on energy and atomic number of the absorber material is calculated at each slice and the probability of a nuclear event in the slice is calculated. A random number is drawn from a uniform distribution and compared to the probability, thus determining whether or not a nuclear event has taken place. This approach will be correct as long as the probability is less than one, as no more than one scattering per slice is considered. Any nuclear event is either elastic or inelastic, as determined by another random number which is compared to the ratio of inelastic to elastic cross section. Like for multiple scattering the elastic scattering angle is then projected on the x', y' plane and added to the particle's coordinates. At present kinematic energy loss is not implemented. The A dependence of the total cross section is implemented by scaling the proton-proton cross section at relatively high energy (≈ 50 GeV), where the energy dependence is small, with an empirical function that describes the measured proton-nucleus cross section for many nuclei well (Fig. 1). The energy dependence is

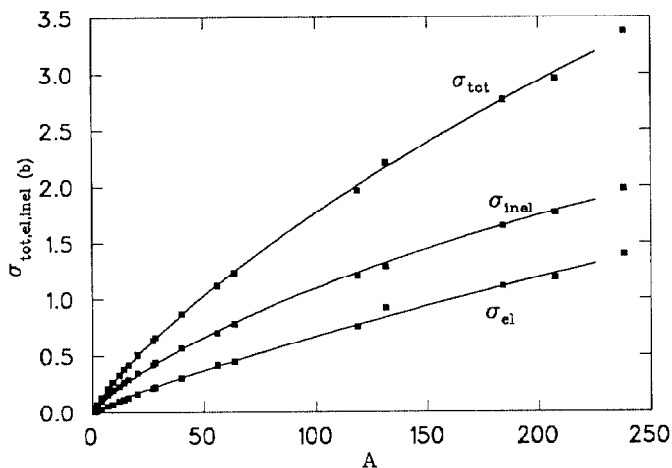


Figure 1: A dependence of the nuclear cross section. The solid lines represent least-squares fits to the data points.

taken to be the same as that of the proton-proton cross section, which again is parametrized with an empirical function (Fig. 2). For the inelastic or reaction cross section the same approach is taken, although this may lead to an underestimate of inelastic events for nuclei as the inelastic cross section becomes significant at much lower energies in p-nucleus scattering than in p-p scattering. For this reason an option is available keeping the inelastic cross section fixed at its high-energy value. All experimental cross section data have been taken from Ref. [6].

The whole scattering and energy loss calculation is repeated for each slice until one of the following occurs:

1. The energy loss calculated is equal to or higher than the current kinetic energy of the particle, minus a lower threshold of 1 MeV, in which case the proton is considered lost and is no longer tracked;

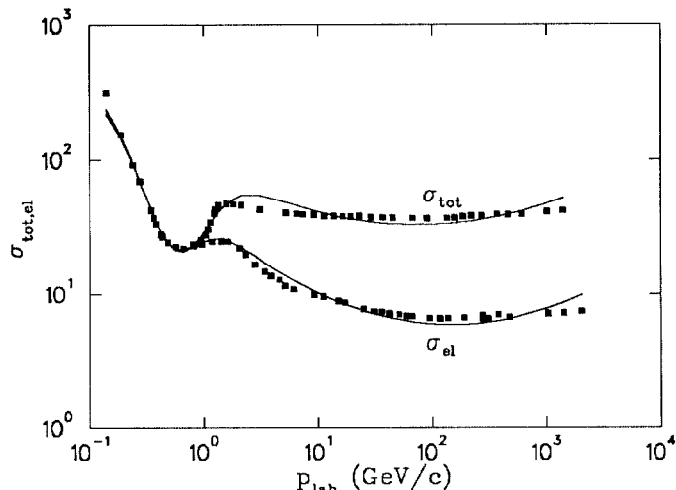


Figure 2: Energy dependence of the proton-proton cross section. The solid lines represent least-squares fits to the data points.

2. The proton undergoes an inelastic nuclear event in which case it is considered lost and is no longer tracked;
3. In either moving to the middle of a slice or finishing a slice the proton leaves the absorber. In this last slice it loses energy only for the length of path in the slice. Once it leaves the block it is moved in a straight line (there is no field in the collimating area) to the end of the collimator or until it enters the other absorber;
4. The proton travels to the end of the absorber without being outscattered or absorbed;
5. The proton moving transversely in the absorber passes a depth (which is a parameter of the element) considered to be the outer side of the absorber. The particle is then no longer tracked.

III. COLLIMATOR SIMULATION FOR THE KAON FACTORY BOOSTER

The routines described above have been used to simulate the collimation system for the Booster of the proposed TRIUMF KAON Factory. The layout of the collimation system is shown in Fig. 3. Collimation in each plane is done in two different straight sections in the same sextant of the ring. Each primary collimator ($cx1$ and $cy1$) is followed by two secondary collimators (cxv and $cx2$, cyh and $cy2$) as particles scattered off the primary collimators have divergences in both planes. Copper (Cu) absorbers of length 0.5 m and tungsten (W) absorbers of length 0.25 m have been considered, the latter being of advantage due to its higher specific mass and thus lower outscattering rate. In both cases the length is about twice the range of protons at 0.45 GeV. Thus the absorbers will become transparent only at energies of about 1 GeV. Placing the secondary collimators in the same drift section as the primary collimator turned out to be essential, otherwise the

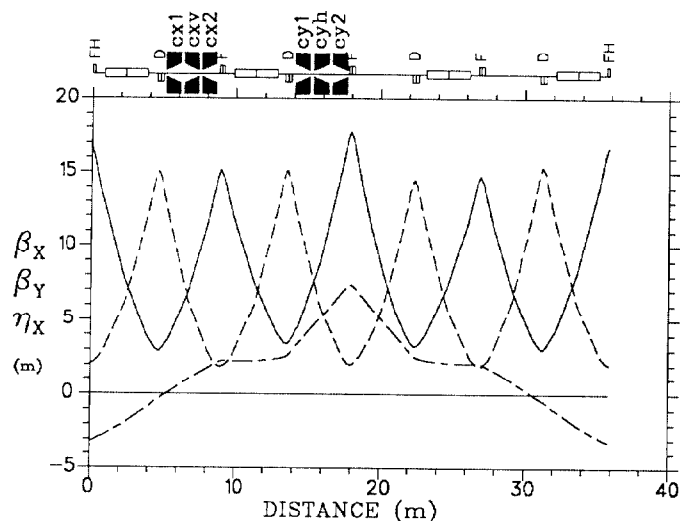


Figure 3: Lattice functions and location of the collimators in the Booster lattice.

magnet following the primary collimator faces heavy irradiation from the outscattering off the primary collimator. The primary collimators define an acceptance of the ring of about 90π mm-mrad, compared to the acceptance of the vacuum system of about 130π mm-mrad. The nominal $2\text{-}\sigma$ beam emittance is 45π mm-mrad at injection.

The loss collection-efficiency of the Booster collimation system is shown in Fig 4 as a function of energy, for both materials. Only kinetic energies up to 1 GeV are considered as most of the losses are expected to occur at lower energy in the Booster. For Cu absorbers an overall efficiency of about 80% is found, while with the tungsten absorber about 90% collection efficiency can be achieved. This increase in collection efficiency stems from a reduced outscattering rate of the tungsten absorbers as shown in Fig. 5, where outscattering of a $1\mu\text{m}$ wide parallel beam from a long absorber as a function of depth of incidence is shown for both materials. For grazing incidence on the face

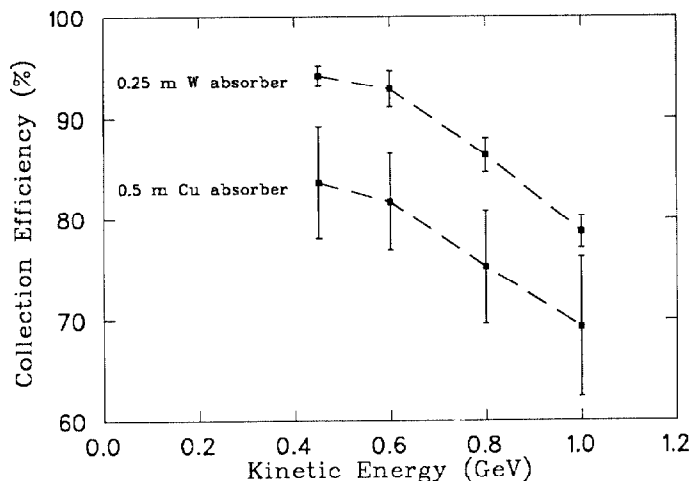


Figure 4: Loss-collection efficiency for W and Cu collimators.

of the collimator, no such dependence was found, however.

The distribution of losses around the ring, assuming Cu absorbers, shows that most losses in the ring are concentrated in the collimation sextant, closely following the collimators, and only a very small part (about 2% of all particles taken out of the beam) is lost elsewhere in the ring. While thus most parts of the ring will be kept "clean", the ramifications for the ring elements close to the collimators in terms of radiation dose have still to be examined. For tungsten absorbers the distributed losses are reduced by a factor of 2.

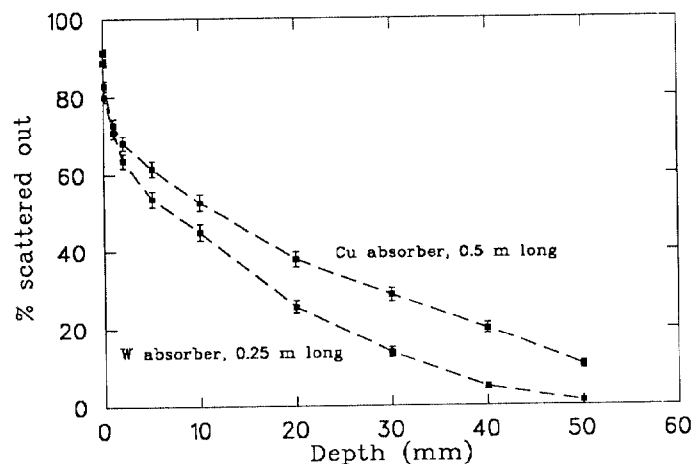


Figure 5: Outscattering for W and Cu absorbers.

IV. ACKNOWLEDGEMENTS

The authors wish to acknowledge helpful suggestions made by D. Measday, UBC, and their colleagues G.H. Mackenzie and I. Thorson at TRIUMF.

V. REFERENCES

- [1] R.V.Servranckx et al., "Users Guide to the Program DIMAD", SLAC Report 285 UC-28 (A), (1985).
- [2] F.W. Jones, "Collimators in ACCSIM", TRIUMF Report TRI-DN-90-K152, Vancouver, B.C. (1990).
- [3] G. Jarlskog and L. Jönsson, "Monte-Carlo Generation of Multiple Scattering of Particles (MLR)", CERN Program Library, W601 (1973).
- [4] B. Schorr, "Programs for the Landau and the Vavilov Distributions and the Corresponding Random Numbers", CERN Program Library, G110/G111, (1974).
- [5] T.Risselada, "Multiple Scattering And Collimation Of Proton Beam At The ISR", CERN Report ISR-OP/77-16. Geneva (1977).
- [6] Particle Data Group, "Review of Particle Properties", Phys. Lett. **B239**, 1-516 (1990).